

## UV-Induced Crosslinking and Cyclization of Solution-Cast Polyacrylonitrile Copolymer

Marlon S. Morales, Amod A. Ogale

Department of Chemical Engineering, and Center for Advanced Engineering Fibers and Films, Clemson University, Clemson, South Carolina 29634-0910

Correspondence to: A. A. Ogale (E-mail: ogale@clemson.edu)

**ABSTRACT:** An alternative, rapid stabilization route for polyacrylonitrile (PAN) precursors is reported based on UV-induced crosslinking and cyclization reactions. Two mechanisms of photoinitiation were investigated: homolytic cleavage and hydrogen abstraction. Solution-cast PAN copolymer samples were irradiated for different durations (100, 300, and 600 s) and temperatures ( $\sim 65$  and  $100^\circ\text{C}$ , below and above glass transition temperature respectively). FTIR spectra show the formation of carbon–oxygen, carbon–nitrogen, and carbon–carbon double bonds ( $1450\text{--}1700\text{ cm}^{-1}$  region) attributed to the development of cyclized structure. Conversion indices estimated from the FTIR spectra indicate samples containing hydrogen abstraction photoinitiator show higher extents of cyclization among the three main set of samples. This observation was also confirmed by higher gel percentages measured on the same set of samples. FTIR conversion indices of samples UV-treated above glass transition temperature were higher compared with that for the same specimens UV-treated below glass transition temperature. DSC results show that samples containing hydrogen abstraction photoinitiator enable a higher extent of post-UV thermal cyclization. FTIR spectra of the UV treated samples were compared with conventional thermal stabilized specimens. This comparison confirms that the addition of 1 wt % photoinitiator to PAN followed by 5 min of UV treatment increases the rate of the cyclization reaction and reduces the thermal oxidation time by over an hour, which could significantly reduce the conventional stabilization time by half. These results indicate the potential for an energy-efficient, cost-effective route for producing carbon fibers. © 2012 Wiley Periodicals, Inc. *J. Appl. Polym. Sci.* 000: 000–000, 2012

**KEYWORDS:** polyacrylonitrile; photochemistry; stabilization; crosslinking; properties and characterization; FTIR; gel percentage; DSC

Received 18 May 2012; accepted 26 July 2012; published online

DOI: 10.1002/app.38398

### INTRODUCTION

Polyacrylonitrile (PAN)-based carbon fibers possess outstanding mechanical strength, and have found numerous applications in ultrahigh performance applications.<sup>1</sup> These fibers have a low density of about  $1.8\text{ g cm}^{-3}$  and can provide energy efficiency in the civilian aeronautical, energy generation, and sports applications, if their cost can be reduced.<sup>2</sup> A rate-limiting step in the conversion of PAN-based precursors into carbon fibers is the stabilization step. Thermo-oxidative stabilization typically involves the heating of the polymer precursor fibers in the range between  $200$  and  $300^\circ\text{C}$  in air or in another oxidizing atmosphere.<sup>3–5</sup> This heat treatment involves the conversion of the PAN polymer chains into a condensed ring structure with a carbon–nitrogen double bond often known as a “ladder” structure.<sup>6</sup> This is considered the most critical step during the production of carbon fibers because it determines the final structure and mechanical properties of the resulting carbon fibers.<sup>7,8</sup>

The thermo-oxidative reactions in PAN are highly exothermic.<sup>1,7</sup> Further, thermal conductivity of PAN precursor (like other polymers) is relatively small ( $\sim 0.26\text{ W m}^{-1}\text{ K}^{-1}$ ).<sup>9</sup> Thus, the rate of heat dissipation during the stabilization is a rate-limiting step. If the heat of reaction is not adequately removed in a real process, the core of the fibers can degrade and result in poor final mechanical properties of the carbon fibers.<sup>10–12</sup>

Reducing the rate of reaction and the temperature of initiation of the exothermic reactions can be used to control the heat flux of the fiber during the thermal oxidation step. This is one of the reasons for the use of copolymers of PAN with a low percentage of comonomer such as methyl acrylate (MA), acrylic acid (AA), or itaconic acid (IA). These comonomers disrupt the order in PAN leading to a reduction of the temperature of initiation of the cyclization reactions producing carbon fibers with higher mechanical properties than carbon fibers produced from PAN homopolymer.<sup>13</sup> Literature studies have discussed interesting piezo-optic response in photopolymers.<sup>14</sup> The acoustic–

optic interaction may provide yet another mechanism for manipulating chemical changes and rates within photopolymers.

PAN-based terpolymer containing a photo sensitive comonomer, such as acryloyl benzophenone, have been investigated and successfully converted into carbon fibers in previous studies.<sup>15</sup> In addition, polymerization and stabilization reactions are known to proceed at lower temperatures when initiated by UV radiation.<sup>16,17</sup> Reduced cyclization temperature can also help to maintain molecular orientation during thermal oxidation, which in turn is important to impart superior modulus and strength properties to the resulting carbon fibers.<sup>8,18–20</sup> Alternatively, the incorporation of this UV-based preoxidation step may lead to a reduction of the time required for thermal stabilization process while maintaining the properties of resulting fibers.

Therefore, the overall goal of this research was to investigate UV-assisted stabilization reactions for PAN precursors. The fundamental study reported here investigates the crosslinking and cyclization reactions in solution-cast PAN samples induced by the addition of photoinitiators that generate free radicals by two different mechanisms, namely, homolytic cleavage and hydrogen abstraction.

## EXPERIMENTAL

### Materials

Poly(acrylonitrile-*co*-methylacrylate) with a nominal AN/MA ratio of 94 : 6 and glass transition temperature ( $T_g$ ) of  $\sim 82.5^\circ\text{C}$  was used throughout this study. Two different photoinitiators, 1-hydroxycyclohexyl phenyl ketone (denoted as “HPK”) and 4,4'-bis(diethylamino)benzophenone (denoted as “DBP”), were used during this study, as shown in Figure 1. HPK generates free radicals by homolytic cleavage mechanism and has UV absorbance peak at 244 nm in the UVC region (250–260 nm). In contrast, DBP does so by hydrogen abstraction and has UV absorbance peak at 378 nm in the UVA region (320–390 nm).<sup>21–23</sup> The solvent used for solution-casting of polymer film samples was dimethyl sulfoxide (DMSO). All materials were obtained from Sigma–Aldrich (Aldrich Chemical Company, Milwaukee, WI) and were used as received.

### UV-Treatment of Samples

The PAN-based precursor and photoinitiator were dissolved in DMSO at  $70^\circ\text{C}$ . The amount of solids in solution was kept at  $\sim 15$  wt %. Films were cast from solution and dried at  $70^\circ\text{C}$  in a conventional oven for  $\sim 24$  h in air. The final thickness of the films was  $\sim 20$   $\mu\text{m}$ . To generate control samples, no photoinitiator was added; the remaining procedure was identical to the one used with the photoinitiator. The films were irradiated with a Nordson 4.5 kW UV curing lamp (Model: 111465 A) having a mercury bulb radiation source (bulb model: PM1163). Mercury bulbs are the most widely used UV source, and were used throughout this study. The intensity of the mercury bulb was measured using a high energy UV radiometer (Electronic Instrumentation and Technology). Intensity values of  $\sim 0.228$ , 0.196, 0.032, and 0.095  $\text{W cm}^{-2}$  were measured for the UVA, UVB, UVC, and UVV ranges, respectively. Films were irradiated for 100, 300, and 600 s. The distance between the samples and the UV source was kept constant at  $\sim 20$  cm. A custom-built

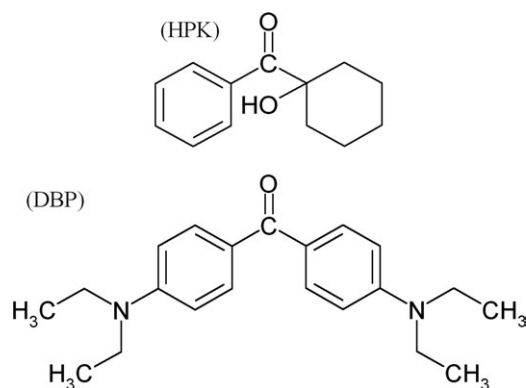


**Figure 1.** 1-Hydroxycyclohexyl phenyl ketone (denoted as “HPK”) and 4,4'-bis(diethylamino)benzophenone (denoted as “DBP”) photoinitiators used throughout the study.

air cooling system was placed inside the UV chamber to remove the excess of heat generated by the source during the UV-treatment. Thus, temperature was controlled during each experiment to study the reactions in two different regimes, 65 and  $100^\circ\text{C}$ , that are respectively below and above the  $T_g$  of the precursor. All UV treated samples were compared against two types of control films. The first control consisted of pure as-produced PAN film. The second control consisted of samples that were covered by a metal sheet (to avoid UV exposure) but ones that were treated in the same UV chamber to provide similar thermal exposure.

Finally, PAN samples were only thermo-oxidative stabilized (as in conventional processes) to produce control samples whose extent of cyclization could be compared with those of the UV-treated samples. The samples were placed on metal frames and heated at  $2.5^\circ\text{C min}^{-1}$  to  $320^\circ\text{C}$  and held there for 30 min. During this thermal oxidation, samples were removed from the oven at 150, 175, 200, 212.5, 225, 240, 255, 270, 280, 300, 320, and  $320^\circ\text{C}$  (after 30 min) to analyze and quantify the partial extent of the cyclization reaction.

### Characterization

Fourier transform infrared spectroscopy (Nexus 870 FT-IR ESP, Nicolet) was used to determine the chemical changes induced during the UV treatment and estimate the extent of the cyclization reaction. Peaks located in the double bond region between 1450 and 1700 wavenumbers ( $\text{cm}^{-1}$ ) are associated with the ladder structure.<sup>7,24–26</sup> The scans were conducted from 400 to  $4000\text{ cm}^{-1}$  and the transmittance intensities were normalized against the intensity of the  $2940\text{ cm}^{-1}$  peak ( $\text{CH}_2$  asymmetric stretching) for comparison. The extent of the cyclization reaction was estimated from the following conversion index<sup>10,27,28</sup>:

$$\text{Conversion index (\%)} = \frac{I_{1600}}{I_{2240} + I_{1600}} \times 100\%$$

where  $I_{1600}$  is the measured intensity of the peak located at  $\sim 1600\text{ cm}^{-1}$ , which corresponds to carbon–nitrogen double bonds associated with the heterocyclic ring structure or ladder structure developed during the thermal oxidation of the PAN-based precursors.  $I_{2240}$  corresponds to the measured peak

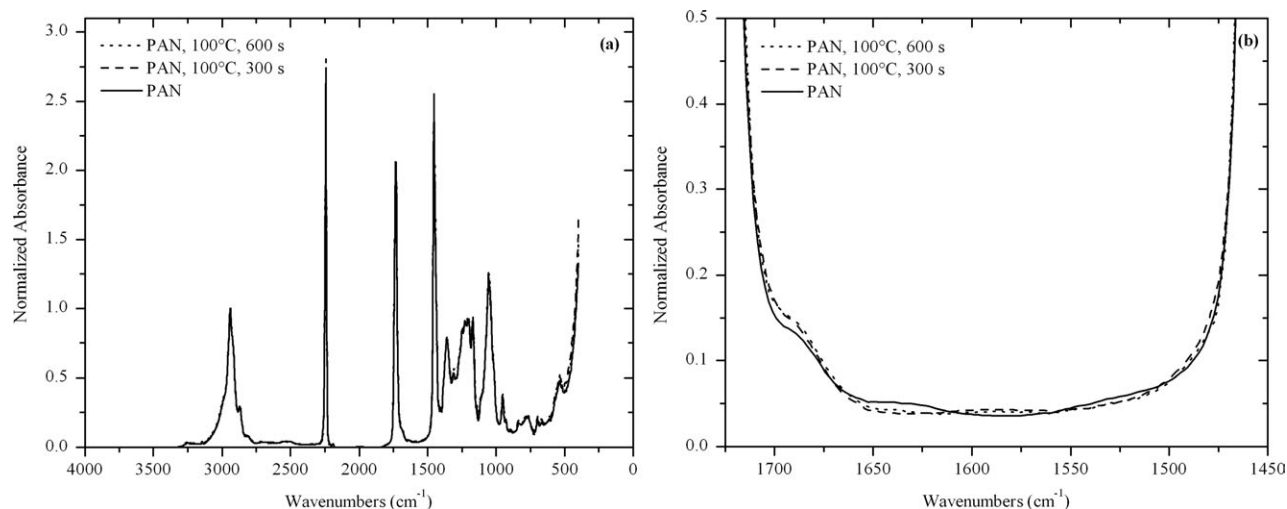


**Figure 2.** FTIR spectra of as-produced PAN and two non-UV exposed but thermally treated control samples at 100°C for 300 and 600 s: (a) over extended wavenumbers, and (b) zoomed-in spectra over the double bond region.

intensity of the peak located at  $\sim 2240\text{ cm}^{-1}$  associated to the carbon–nitrogen triple bond present in the original polyacrylonitrile structure. The peak intensities values used to calculate these conversion indexes were raw intensity values given by the FTIR spectrometer without any normalization.

The gel content (insoluble material) is proportional to the extent of cyclization and crosslinking reactions undergone by the samples during the UV treatment. Approximately 100 mg of treated sample was immersed in about 10 mL DMSO and allowed to dissolve at 70°C for over 48 h under constant agitation. The gel was then separated from the solution using a pre-weighed filter paper, dried in a vacuum oven at 70°C, and the remaining gel mass was measured using a microbalance. The gel fraction of each sample was calculated as the ratio of the remaining insoluble mass and the initial mass of film used in the analysis.<sup>16,29</sup>

Differential scanning calorimetry (Pyris 1 DSC, Perkin Elmer Instruments) was conducted to observe the thermal behavior of the samples after being UV-treated and to quantify the residual heat that a UV-treated sample would liberate upon further conventional thermal oxidation. Approximately 4 mg of film sample was heated up to 350°C at a rate of  $5^\circ\text{C min}^{-1}$  in air environment. For each of the characterization techniques used during this study, at least three different measurements were conducted on the different samples.

## RESULTS AND DISCUSSION

### Influence of Photoinitiator

Figure 2(a) displays the FTIR spectra of three control specimens: as-produced PAN and two non irradiated but thermally treated samples at 100°C for 300 and 600 s. These correspond to the longest treatment times for each set of samples discussed in the following sections. In Figure 2(b), the section between  $\sim 1450$  and  $\sim 1700\text{ cm}^{-1}$  displays the double bond region associated with the carbon–oxygen, carbon–nitrogen, and carbon–carbon double bonds present in the ladder structure. This region

includes the most significant differences among all the FTIR spectra. The peaks located at 2940, 2865, 2242, 1730, 1454, and  $1055\text{ cm}^{-1}$  have been assigned to  $\text{CH}_2$  asymmetric stretching,  $\text{CH}_2$  symmetric stretching,  $\text{C}\equiv\text{N}$  stretching,  $\text{C}=\text{O}$  stretching (due to the presence of methyl acrylate),  $\text{CH}_2$  scissor vibration, and  $-\text{C}-\text{C}-\text{C}-$  backbone bending, respectively.<sup>7,16,24,25,29</sup> These results confirm that simply raising the temperature in the UV-chamber has no discernible effect on the chemical modification of the nonirradiated samples.

Figure 3 displays FTIR spectra obtained from samples UV treated at 100°C for 300 s, with and without photoinitiators. It is evident that the intensities of this double bond region were higher for UV-treated samples containing 1 wt % DBP (hydrogen abstraction photoinitiator) as compared with samples containing 1 wt % HPK (homolytic cleavage) or the controls (pure, UV treated). The conversion index was calculated for each set

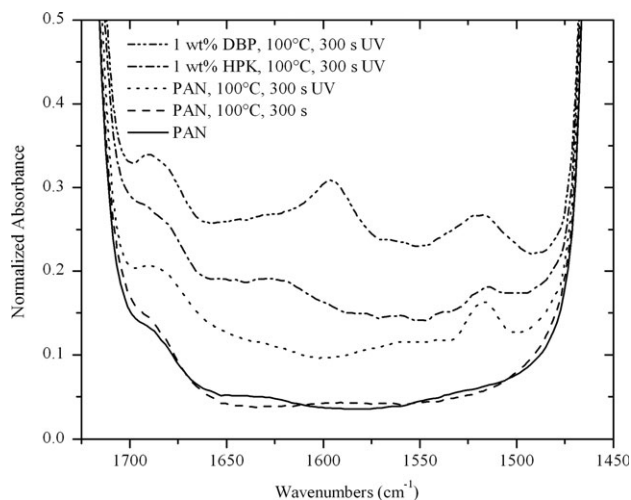


**Figure 3.** FTIR results of PAN-based copolymer containing 1 wt % DBP, 1 wt % HPK and without photoinitiator; UV treated at 100°C for 300 s; compared against as-produced and thermally treated control samples.

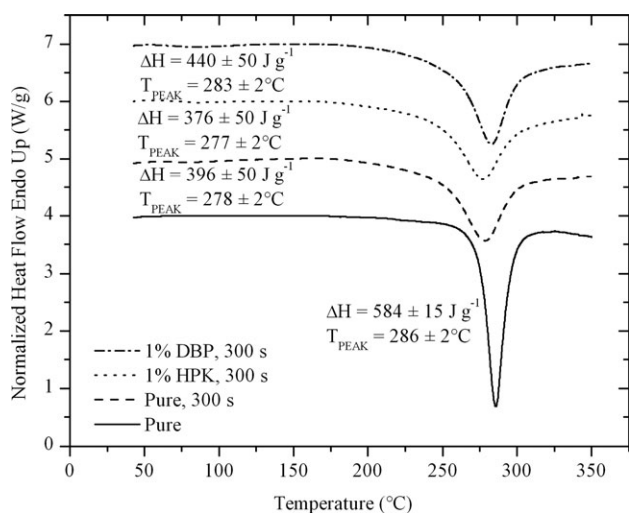


**Figure 4.** DSC scans of PAN copolymer with and without photoinitiator UV-treated at 100°C for 300 s.  $\Delta H$  represents the residual heat of cyclization.

of samples at  $9.0\% \pm 1.5\%$ ,  $4.6\% \pm 1.5\%$ ,  $2.2\% \pm 1.1\%$ ,  $0.1\% \pm 0.2\%$ , and  $0\% \pm 0.2\%$  for samples containing 1 wt % DBP, 1 wt % HPK, UV-treated pure, and the two control samples, respectively. At 95% confidence, the conversion index was higher for UV treated samples containing 1 wt % DBP (hydrogen abstraction) compared with other samples containing 1 wt % HPK (homolytic cleavage PI) and UV-treated pure samples. Thermally treated samples without UV exposure show no ladder formation. Hence, the presence and type of photoinitiator influences the extent of cyclization of the samples.

Gel contents of these samples were measured at  $59\% \pm 10\%$ ,  $42\% \pm 10\%$ , and  $25\% \pm 10\%$  for specimens containing 1 wt % DBP, 1 wt % HPK, and pure UV-treated films at 100°C for 300 s, respectively. As expected, the control samples did not produce any gel. These gel fraction measurements are in good agreement with the behavior described by the FTIR results in that samples containing 1 wt % DBP (hydrogen abstraction photoinitiator) are more reacted as compared with the one containing 1 wt % HPK (homolytic cleavage photoinitiator) and pure UV-treated sample. These results also confirm that UV-sensitive components can be physically added into the precursor, and not have to be present in the polymer backbone.

The greater double bond formation during UV treatment afforded by the hydrogen abstraction mechanism (over that by homolytic cleavage) can be attributed to the competition between the PAN-based precursor and the photoinitiator. It is known that mercury lamps provide a broad-band output distribution in the UVA, UVB, UVC, and UVV regions.<sup>30</sup> PAN has an UV absorption peak in the UVC region ( $\sim 274$  nm), which falls in the same UV absorption region as do most of photoinitiators dissociating by homolytic cleavage.<sup>21,23</sup> Specifically, HPK has a UV absorption peak at  $\sim 244$  nm. Thus, the PAN-based precursor and photoinitiator compete for the same region of the UV spectrum, and energy absorption is inefficient. On the other hand, hydrogen abstraction-type photoinitiators have UV absorption bands at higher wavelengths in the UVA region, spe-

cifically  $\sim 378$  nm for DBP.<sup>21</sup> This reduces the competition between the PAN-based precursor and photoinitiator for the same region of the UV spectrum. This establishes that hydrogen abstraction photoinitiators offer a more efficient mechanism, as compared to homolytic cleavage type for UV-induced reactions in PAN-based precursors.

Figure 4 displays the DSC results of the residual heat of reaction for PAN-based precursor, with and without photoinitiator, UV-treated at 100°C for 300 s. The exothermic heat of reaction observed is a measure of further thermal oxidation that the sample can undergo. It is evident from the results that UV-treated samples display a reduction in the residual heat of cyclization, which may possibly be attributed to three phenomena occurring during the UV-treatment of the precursor: cyclization, crosslinking, and scission of the polymer chains.<sup>15,16,19,31,32</sup> This reduction of the residual heat of reaction of UV treated specimens as compared with samples without UV treatment means that some reaction has already taken place during UV irradiation, albeit at a lower temperature. Interestingly, specimens containing 1 wt % DBP (hydrogen-abstraction PI) show higher heat of reaction compared with that displayed by samples containing 1 wt % HPK (homolytic cleavage PI) and pure UV-treated samples. Thus, samples containing 1 wt % DBP will undergo additional thermal cyclization during the further thermal oxidation step, which is desired, even though the same specimens also had displayed higher FTIR double bond conversion percentage and gel content. Thus, DBP is able to absorb more UV energy delivered by the source to react with the PAN-based precursor increasing double bond formation. At the same time, reduction of chain scission and crosslinking, which hinder ladder formation during the further thermal oxidation step is observed. By the selection of a suitable photoinitiator, the undesired side reactions (viz. chain scission and crosslinking) can be reduced to favor ladder formation. Because DBP offered a better performance, it was further investigated with regards to different exposure temperatures and durations.

#### Influence of UV Radiation Time and Temperature (above and below $T_g$ )

Figure 5(a, b) displays FTIR spectra of PAN-based copolymer without any photoinitiator [Figure 5(a)] and with 1 wt % DBP [Figure 5(b)]. Both set of samples were UV treated at 100°C for 100, 300, and 600 s and are compared with as-produced and thermally treated control samples. The conversion indexes were measured to be  $6.2\% \pm 1.5\%$ ,  $9.0\% \pm 1.5\%$ , and  $15.2\% \pm 1.5\%$  for samples containing 1 wt % DBP UV treated for 100, 300, and 600 s, respectively. In contrast, the conversion indexes of pure samples were  $0.6\% \pm 1.1\%$ ,  $2.2\% \pm 1.1\%$ , and  $7.3\% \pm 1.5\%$  for the three durations. For both set of samples, increased UV exposure time led to higher double bond formation and higher conversion index in the double bond region. These results are consistent with prior studies that show that PAN precursors can be cyclized by high-intensity UV radiation.<sup>15,19</sup> The cyclized polymer can subsequently be thermally stabilized for successful conversion into carbon fibers.<sup>16</sup> Although there is some evidence of cyclization reaction occurring in UV-treated samples without PI, the double bond region intensity is significantly higher for samples containing photoinitiator.

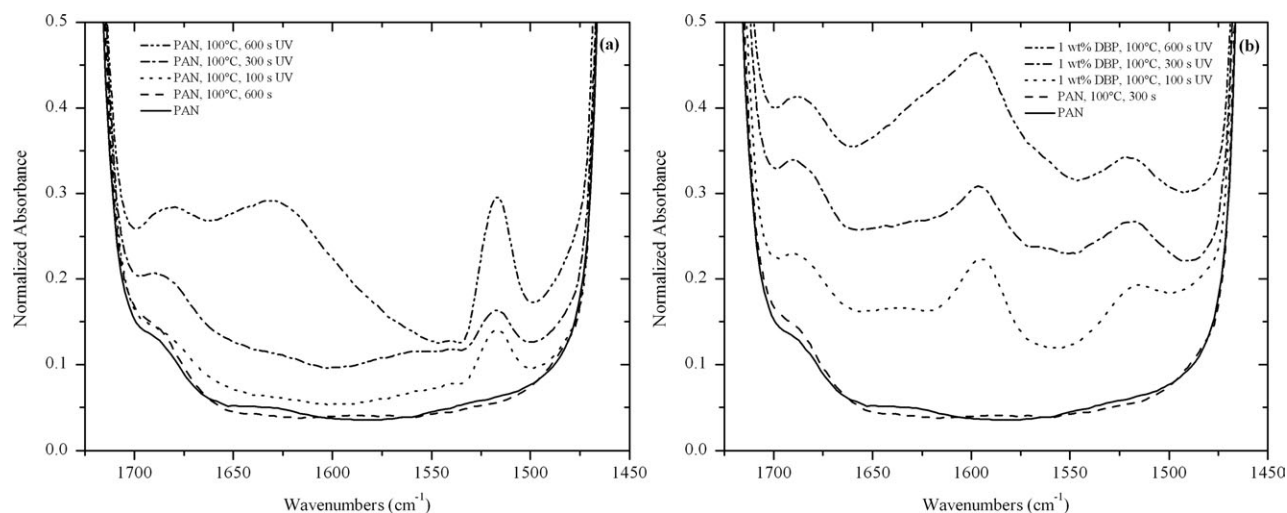


**Figure 5.** FTIR analysis of PAN-based copolymer with and without photoinitiator UV treated at 100°C for 0, 100, and 600 s: (a) without photoinitiator, and (b) with 1 wt % DBP; compared against as-produced and thermally treated control samples.

In addition to the different intensities observed for the different samples, two other differences were observed. Samples without PI show three noticeable peaks located at 1680, 1630, and the clearest at 1520  $\text{cm}^{-1}$ . In contrast, samples containing 1 wt % BDP has an extra peak located at 1600  $\text{cm}^{-1}$ . This peak is very clear for samples containing PI after UV treatment for only 100 s, and it is not significant for samples without PI even after 600 s of UV treatment. It is known that radicals are more likely to add to unsaturated groups, such as the nitrile group present in the PAN structure.<sup>16,31,32</sup> Thus, it is believed that the generated photoinitiator radicals react with the carbon–nitrogen triple bonds to start the radical cyclization reaction. The peak located at 1600  $\text{cm}^{-1}$ , clearly observed for samples containing PI, has been assigned to the carbon–nitrogen double bond. The presence of the 1520, 1600, 1630, and 1680  $\text{cm}^{-1}$  peaks is a clear indicator of the formation of the ladder structure after the UV treatment.<sup>7,24–26</sup>

In contrast, due to the absence of photoinitiator in pure samples, dehydrogenation reaction is believed to be the primary pathway during UV treatment. Hydrogen radicals produced during the UV-treatment combine to form hydrogen, with carbon–carbon double bond formation in the back bone of the precursor or even crosslinking and scission of the polymer chains, presumably in the amorphous region.<sup>19,31,32</sup> Based on these arguments, the two peaks located at 1630 and 1520  $\text{cm}^{-1}$  (the clearest and most intense for UV-treated samples without PI) are believed to be associated with the conjugated carbon–carbon double bond system. The peak located at 1680  $\text{cm}^{-1}$  has been assigned to the carbon–oxygen double bond formation. Although these are the most noticeable peaks, these overlap with other weaker peaks associated with the ladder structure. Conjugated carbon–oxygen and carbon–nitrogen double bonds, carbon–carbon and carbon–nitrogen single bond stretching, and NH in-plane bending have been assigned in the region between

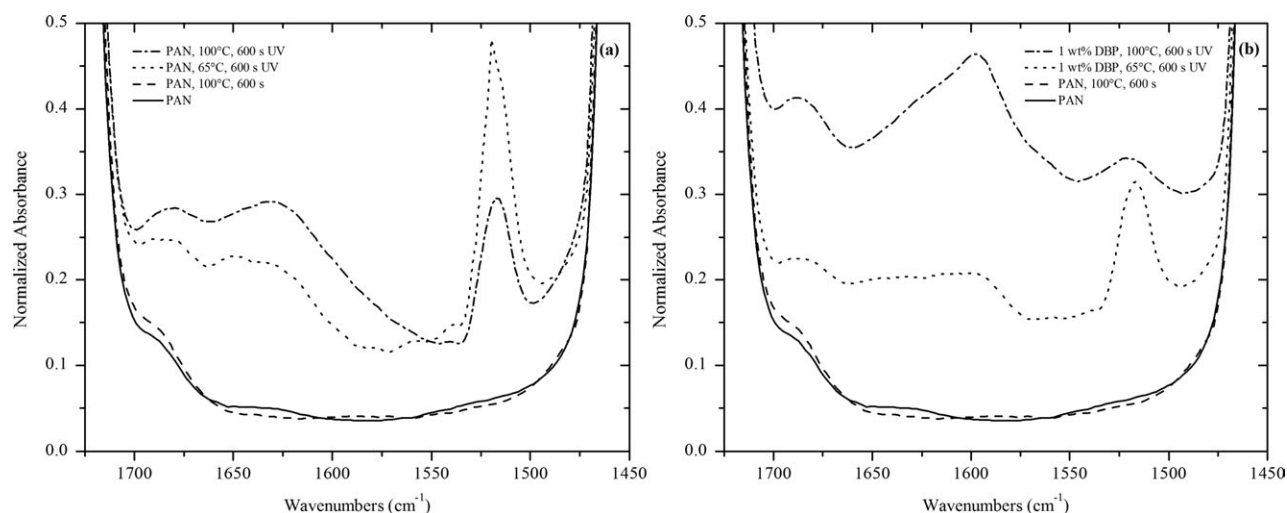


**Figure 6.** FTIR analysis of PAN-based copolymer UV treated at 65 or 100°C for 600 s: (a) without photoinitiator, and (b) with 1 wt % DBP; compared against as-produced and thermally treated control samples.

1500 and 1700  $\text{cm}^{-1}$ .<sup>7,24</sup> The presence of photoinitiator affects the extents and how favorable a specific reaction can become over other parallel reactions taking place during the UV treatment of the PAN-based precursors.

To study the effect of polymer mobility on the photo-induced cyclization of PAN-based specimens with and without photoinitiator, samples were UV treated below and above the  $T_g$  of the PAN-based precursor. Figure 6(a, b) summarizes these results. Figure 6(a) shows PAN-based specimens without photoinitiator UV-treated at 65 or 100°C for 600 s. These two temperatures are below and above the glass transition temperature of the PAN-based copolymer ( $T_g \sim 82.5^\circ\text{C}$ ), respectively. Figure 6(b) displays another set of samples containing 1 wt % DBP UV treated at the same temperatures of the pure precursor. The conversion indexes of the samples without photoinitiator UV treated at 65 and 100°C were  $4.7\% \pm 1.5\%$  and  $7.3\% \pm 1.5\%$ . For samples containing 1 wt % DBP the indexes were  $6.8\% \pm 1.5\%$  and  $15.2\% \pm 1.5\%$ , respectively. In both set of samples, specimens UV-treated above  $T_g$  of the precursor show higher intensities in the double bond region compared with that for the samples UV-treated below  $T_g$ . The presence of photoinitiator plays a bigger role on the extent of the ladder structure formation on samples UV-treated above  $T_g$  (7.3% vs. 15.2%) compared with the values obtained for samples UV-treated below the  $T_g$  of the precursor (4.7% vs. 6.8%).

These results can be explained by the fact that the mobility of the polymer chains is limited below the  $T_g$  of the precursor, which reduces the reactivity of the precursor. Based on the similarities shown by their respective FTIR spectra, the presence of photoinitiator has little effect on the type of reactions undergone by the samples UV treated at temperatures below the  $T_g$  of the precursor. In both set of samples, with and without photoinitiator UV-treated below  $T_g$ , a very prominent peak at 1520  $\text{cm}^{-1}$  mainly associated with carbon-carbon conjugated double bonds is observed. The only subtle difference observed between these two spectra is the wider shoulder shown by the sample containing photoinitiator reaching the 1600  $\text{cm}^{-1}$  region, which is associated with carbon-nitrogen double bond present in the ladder structure. Although some carbon-nitrogen double bond formation is observed for samples containing photoinitiator UV-treated below  $T_g$ , the amount of triple bonds attacked by the photoinitiator radicals during the UV treatment has been reduced by the restricted polymer chain mobility. As discussed earlier, samples containing photoinitiator and UV treated above  $T_g$  show higher double bond intensity specially the 1600  $\text{cm}^{-1}$  peak related with carbon-nitrogen double bonds. Pure samples are more inclined to form carbon-carbon double bonds when UV-treated irrespective of the temperature. The limited mobility of the polymer chains below  $T_g$  limits the effect of photoinitiator. Thus, processing temperature (relative to precursor  $T_g$ ) and the composition (type of PI) during this photoinduced oxidation process play an important role in achieving the stabilization reaction.

Finally, Figure 7 displays the FTIR spectra of pure PAN-based copolymer at different stages during the traditional thermal oxidation treatment in air. The overall changes involve the

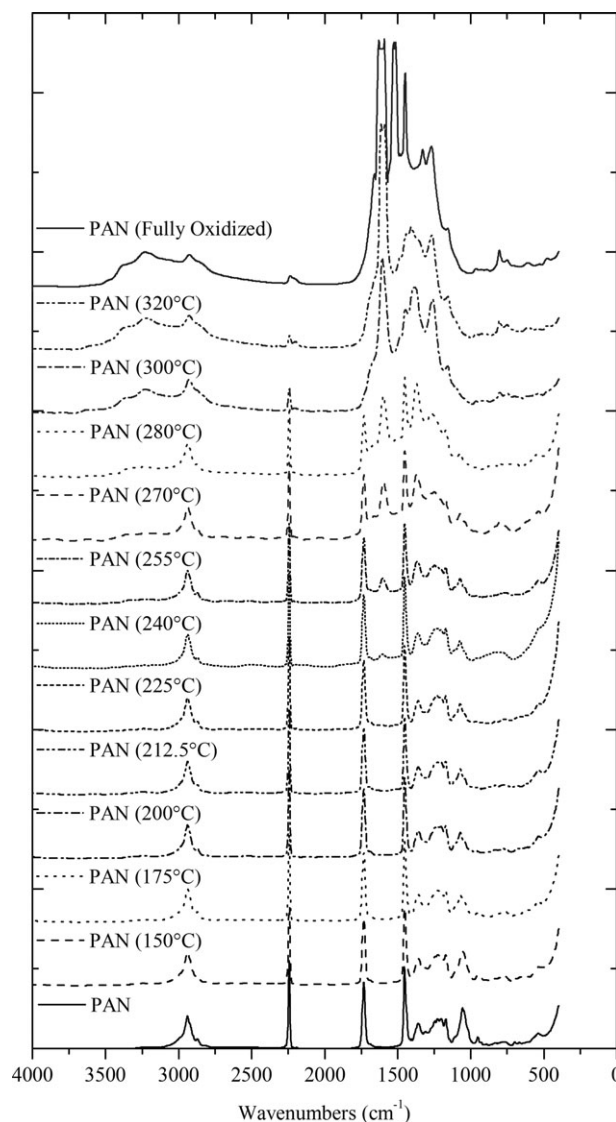


**Figure 7.** FTIR spectra of pure PAN-based copolymer at different stages during the traditional thermal oxidation treatment in air.

reduction of the  $\text{C}\equiv\text{N}$  stretching peak (2242  $\text{cm}^{-1}$ ),  $\text{CH}_2$  stretching peak (2937  $\text{cm}^{-1}$ ),  $\text{CH}_2$  bending peak (2937  $\text{cm}^{-1}$ ), and carbon back bone bending peak (1051  $\text{cm}^{-1}$ ). On the other hand, primary amines (3390 and 3356  $\text{cm}^{-1}$ ), carbon-oxygen double bond (1680  $\text{cm}^{-1}$ ), carbon-nitrogen double bond (1600  $\text{cm}^{-1}$ ), carbon-carbon double bond (1630  $\text{cm}^{-1}$ ), conjugated carbon-carbon double bond corresponding to the heterocyclic ring structure (1520  $\text{cm}^{-1}$ ), carbon-hydrogen in and out of plane deformations (1370 and 805  $\text{cm}^{-1}$ , respectively), and carbon-oxygen single bond (1150  $\text{cm}^{-1}$ ) appear. All these peaks are related to the cyclized structure produced during the thermal oxidation treatment.<sup>7,16,24,25,29</sup>

Figure 8 shows the section between  $\sim 1450$  and  $\sim 1700$   $\text{cm}^{-1}$  of the first four FTIR spectra shown in Figure 7 corresponding to as-produced PAN samples, and those thermally treated up to 150, 175, and 200°C. The four spectra indicate the start of the standard thermally activated cyclization reaction in an oxidizing

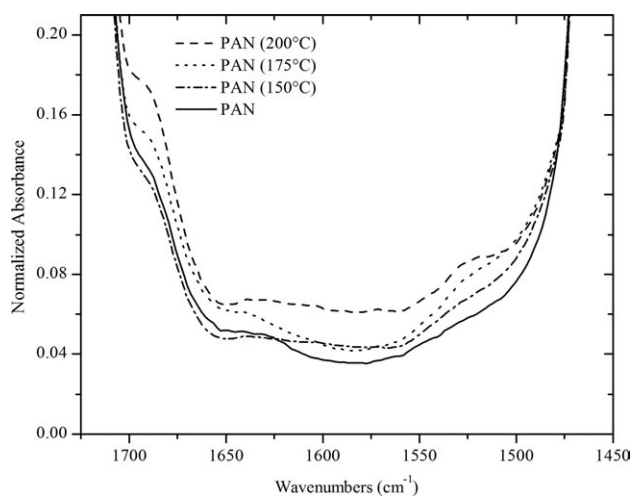


**Figure 8.** FTIR spectra of as-produced PAN-based copolymer and the same sample thermally treated up to 150, 175, and 200°C.

environment. For the PAN copolymer investigated in this work, chemical changes in the double bond region associated with the ladder structure are observed at temperatures between 150 and 175°C. They appear as shoulders of the two strong peaks (1730  $\text{cm}^{-1}$ , methyl acrylate C=O stretching; and 1454  $\text{cm}^{-1}$ ,  $\text{CH}_2$  scissor) belonging to the original PAN copolymer structure. The subtle peaks observed at 175°C belong to the carbon-oxygen double bond (1680  $\text{cm}^{-1}$ ) and carbon-carbon conjugated system (1630 and 1520  $\text{cm}^{-1}$ ). Between 175 and 200°C, the intensity around 1600  $\text{cm}^{-1}$  starts to become noticeable indicating carbon-nitrogen double bond formation associated with cyclization. These observations indicate that the first reaction to take place during the thermal oxidation is the dehydrogenation reaction by oxygen attack on the polymer chains. The cyclization reaction starts immediately after the dehydrogenation reaction initiates. These observations are consistent with those reported in the literature.<sup>11,26</sup> Notice that the reaction path followed by the thermally treated samples is similar to the one followed by the UV treated samples without photoinitiator described at the beginning of this section.

Based on FTIR spectra displayed in Figure 7, the FTIR conversion indices for pure, non-UV treated, thermally stabilized samples are presented in Figure 9 as a function of the thermal stabilization time. Also included is the temperature profile followed during these thermal stabilization experiments. These results show that most of the conversion of the precursor occurs during the second half of the thermal treatment process, specifically between 200 and 300°C. In addition, the dashed line indicates the conversion index of 9.0% for a sample containing 1 wt % DBP UV treated at 100°C for 300 s. The results show that 300 s (5 min) of UV treatment of the PAN-copolymer containing 1 wt % DBP are approximately equivalent to the first 4800 s (80 min) of the thermal oxidation process, i.e., a reduction of approximately half of the time. In addition, during the UV treatment, the sample was kept at 100°C; in contrast, the thermal treated samples have to reach  $\sim 240^\circ\text{C}$  to achieve the same conversion index. Thus, the same conversion was achieved in a shorter period of time at a lower temperature. The conversion

index for UV-treated samples in the absence of photoinitiator was  $\sim 2\%$  and not statistically different from the initial indices for pure PAN samples thermally stabilized (therefore, not included in the figure). These kinetic results indicate the potential for developing a novel and more rapid process for stabilization of PAN-based precursors to produce carbon fibers more efficiently.

## CONCLUSIONS

The effect of UV-photoinitiators and UV-radiation on photo-induced stabilization of polyacrylonitrile was investigated. Hydrogen-abstraction was found to be a more efficient mechanism in comparison with homolytic cleavage during the photo-induced cyclization of PAN precursor polymer. FTIR, gel percentages, and DSC results confirm that samples containing 4,4'-Bis(diethylamino)benzophenone (hydrogen abstraction type) achieved higher extents of cyclization than did samples containing 1-hydroxycyclohexyl phenyl ketone (homolytic cleavage type). Also, the presence of 4,4'-bis(diethylamino)benzophenone enables higher extents of post-UV thermal cyclization. The presence of photoinitiator is more effective in promoting carbon-nitrogen double bond formation for samples UV-treated above the  $T_g$  of the precursor in comparison with UV-treated samples without photoinitiator and samples UV-treated below  $T_g$  where carbon-carbon double bond formation was more favorable. At temperatures below the  $T_g$  of the precursor, the presence of photoinitiator does not play a significant role on the extent of the cyclization due to the limited mobility of the polymer chains. Increasing UV exposure time leads to greater formation and higher FTIR conversion index in the double bond region. The present results confirm that it is possible to produce UV-induced cyclization in PAN-based precursors by the external addition of photoinitiator into the polymer solution (i.e., without necessarily incorporating photoinitiators into the polymer chain itself). Thus, the addition of 1 wt % photoinitiator to PAN and UV treatment for only 5 min increases the rate of the cyclization reaction and reduces the thermal

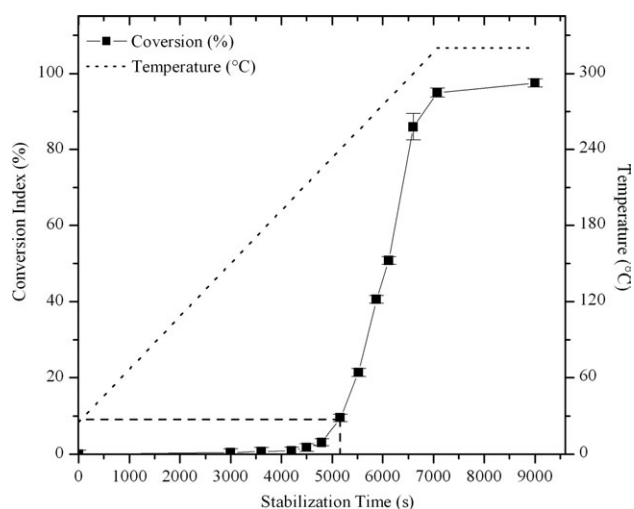


**Figure 9.** Temperature profile and calculated conversion indexes (with trend line) of PAN-based copolymer during the thermal oxidation step.

oxidation time by over an hour, which could significantly reduce the conventional stabilization time by half. These results indicate the potential for an energy-efficient, cost-effective route for producing carbon fibers.

### ACKNOWLEDGMENTS

Financial assistance from AFRL/RXBT (Program Monitor: Dr. Karla Strong) through FA8650-05-D-5807-TO27 is gratefully acknowledged.

### REFERENCES

1. Zhang, W.; Li, M. *J. Mater. Sci. Technol.* **2005**, *21*, 581.
2. Katzman, H. A.; Adams, P. M.; Le, T. D.; Hemminger, C. S. *Carbon* **1994**, *32*, 379.
3. Buckley, J. D. In *Carbon-Carbon Materials and Composites*; Buckley, J. D., Edie, D. D., Eds.; National Aeronautics and Space Administration: Hampton VA, **1992**; Chapter 1, p 1.
4. Diefendorf, R. J. *Engineered Materials Handbook: Composites*; ASM International: Metals Park, OH **1987**; Vol. 1, p 49.
5. Edie, D. D.; Diefendorf, R. J. In *Carbon-Carbon Materials and Composites*; Buckley, J. D., Edie, D. D., Eds.; National Aeronautics and Space Administration: Hampton, VA **1992**; Chapter 2, p 19.
6. Clarke, A. J.; Bailey, J. E. *Nature* **1973**, *243*, 146.
7. Gupta, A.; Paliwal, D.; Bajaj, P. *J. Macromol. Sci. Rev. Macromol. Chem. Phys.* **1991**, *C31*, 1.
8. Wang, P. H.; Yue, Z. R.; Li, R. Y.; Liu, J. *J. Appl. Polym. Sci.* **1995**, *56*, 289.
9. Hou, J.; Wang, X.; Zhang, L. *Appl. Phys. Lett.* **2006**, *89*, 1.
10. Hou, Y.; Sun, T.; Wang, H.; Wu, D. *Text. Res. J.* **2008**, *78*, 806.
11. Hou, Y.; Sun, T.; Wang, H.; Wu, D. *J. Appl. Polym. Sci.* **2008**, *108*, 3990.
12. Yu, M.; Bai, Y.; Wang, C.; Xu, Y.; Guo, P. *Mater. Lett.* **2007**, *61*, 2292.
13. Gupta, D. C.; Agrawal, J. P. *J. Appl. Polym. Sci.* **1989**, *38*, 265.
14. Kityk, I. V.; Kasperczyk, J.; Sahraoui, B.; Yasinskii, M. F.; Holan, B. *Polymers* **1997**, *38*, 4803.
15. Mukundan, T.; Bhanu, V. A.; Wiles, K. B.; Johnson, H.; Bortner, M.; Baird, D. G.; Naskar, A. K.; Ogale, A. A.; Edie, D. D.; McGrath, J. E. *Polymer* **2006**, *47*, 4163.
16. Naskar, A. K.; Walker, R. A.; Proulx, S.; Edie, D. D.; Ogale, A. A. *Carbon* **2005**, *43*, 1065.
17. Decker, C. In *Photochemistry and Polymeric Systems*; Kelly, J. M., Mc Ardle, C. B., Maunder, M. J. de F., Eds.; Royal Society of Chemistry: Cambridge, Great Britain **1993**; p 32.
18. Wu, G.; Lu, C.; Ling, L.; Hao, A.; He, F. *J. Appl. Polym. Sci.* **2005**, *96*, 1029.
19. Paiva, M. C.; Kotasthane, P.; Edie, D. D.; Ogale, A. A. *Carbon* **2003**, *41*, 1399.
20. Wang, P. H. *J. Appl. Polym. Sci.* **1998**, *67*, 1185.
21. Ledwith, A. In *Photochemistry and Polymeric Systems*; Kelly, J. M.; Mc Ardle, C. B.; Maunder, M. J. de F., Eds.; Royal Society of Chemistry: Cambridge, Great Britain **1993**; p 1.
22. Fouassier, J. P. *Prog. Org. Coat.* **1990**, *18*, 229.
23. Fouassier, J. P.; Burr, D.; Wieder, F. *J. Appl. Polym. Sci. A Polym. Chem.* **1991**, *29*, 1319.
24. Shimada, I.; Takahagi, T. *J. Polym. Sci. A Polym. Chem.* **1986**, *24*, 1989.
25. Sun, T.; Hou, Y.; Wang, H. *J. Appl. Polym. Sci.* **2010**, *118*, 462.
26. Fitzer, E.; Müller, D. *J. Carbon* **1975**, *13*, 63.
27. Zhu, Y.; Wilding, M. A.; Mukhopadhyay, S. K. *J. Mater. Sci.* **1996**, *31*, 3831.
28. Dalton, S.; Heatley, F.; Budd, P. M. *Polymer* **1999**, *40*, 5531.
29. Badawy, S.; Dessouki, A. *J. Phys. Chem. B* **2003**, *107*, 11273.
30. Boyd, I. W.; Zhang, J. Y. *Nuclear Instrum. Methods Phys. Res. Sect. B (Beam Interact. Mater. Atoms)* **1997**, *121*, 349.
31. Newton, A. S. In *Radiation Effects on Organic Materials*; Bolt, R. O., Carroll, J. G., Eds.; Academic Press: New York, NY **1963**; Chapter 3, p 35.
32. Hall, K. L.; Bolt, R. O.; Carroll, J. G. In *Radiation Effects on Organic Materials*; Bolt, R. O., Carroll, J. G., Eds.; Academic Press: New York, NY **1963**; Chapter 4, p 63.